Blazed gain grating in a four-level atomic system

Shang-qi Kuang* and Hai-gui Yang

Changchun Institute of Optics, Fine Mechanics and Physics, Chinese Academy of Sciences, Changchun 130033, China
**Corresponding author: physicskuang@sina.com*

Received October 31, 2012; accepted November 14, 2012;
posted November 19, 2012 (Doc. ID 178868); published December 13, 2012

A blazed gain grating in a four-level atomic system is theoretically demonstrated. This grating is based on the spatial modulation of Raman gain, which is created by an intensity mask in the signal field. Due to the modulo-2π phase modulation, the majority of energy in the amplified probe beam can be deflected into the first-order direction, and a diffraction efficiency higher than 100% is predicted. When an intensity mask having two symmetric domains is adopted, this proposal can give a further possibility of all-optical beam splitting. © 2012 Optical Society of America

OCIS codes: 020.1670, 270.1670, 050.2770.

1. INTRODUCTION

Recently, research of atomic gratings based on atomic coherence effects has become a research focus. By replacing the travelling field of electromagnetically induced transparency (EIT) [1] with a standing wave, an electromagnetically induced grating (EIG) is created [2], and this phenomenon has been observed [3]. Since the EIG is created by the spatial modulation of atomic absorption and dispersion of the resonant probe beam, the diffraction efficiency cannot be very high. In order to improve the diffraction efficiency of EIG, several proposals of electromagnetically induced phase grating were reported [4–6], which are based on the periodic modulation of giant Kerr nonlinearity of EIT systems. In this phase EIG, the atomic dispersion can be altered periodically, and low probe absorption can also be maintained, and then the first-order diffraction efficiency of this phase grating can be close to the efficiency of an ideal sinusoidal phase grating. Compared with the atomic gratings based on EIT, a kind of gain-phase grating or gain grating based on active Raman gain (ARG) was also demonstrated [7,8]. Owing to the spatial modulations of Raman gain and Kerr nonlinearity in the ARG system [9–11], the gain-phase grating and gain grating can supply much higher diffraction efficiency in high-order directions. Common to the aforementioned gratings is that the spatial modulation is induced by a standing wave, and the probe beam is diffracted into several high-order directions. When an intensity mask is used in the coupling or signal fields in the EIT systems, a kind of blazed grating with 2π phase modulation is created, and it can deflect the probe beam into a certain order (first-order) direction [12,13]. This blazed grating based on EIT is essentially a phase grating, and its first-order diffraction efficiency, which can approach 100%, is limited by the probe absorption.

In this paper, we theoretically demonstrate a blazed gain grating in an ultracold atomic medium. This blazed gain grating is based on ARG, and it is created by an intensity-modulated mask in the signal field. Owing to the spatial modulations of probe gain and phase, the majority of energy in the amplified probe beam can be deflected into the first-order direction, and then the diffraction efficiency can be higher than 100%. Therefore, the probe beam at low light levels can also be manipulated, and this scheme may have great potential to be utilized as an all-optical switching and routing in the optical networking [14,15]. When a more sophisticated intensity mask that has two symmetric domains is used, our proposal gives a further possibility of all-optical beam splitting for quantum information process.

2. ATOMIC MODEL AND EQUATIONS

We consider a four-level atomic system interacting with three laser fields, as shown in Fig. 1. A pumping field E_p with a large detuning Δ_p drives transition $|3\rangle$–$|1\rangle$. The $|3\rangle$–$|2\rangle$ transition is excited by a weak probe field E with a large detuning Δ, and two-photon detuning of Raman resonance is $\delta = \Delta_p - \Delta$. A signal field E_s connects the transition $|4\rangle$–$|2\rangle$, and it is also far detuned from resonance by Δ_s. We define that Γ_{ij} ($i = 3, 4$; $j = 1, 2$) is the spontaneous decay rate of the corresponding transition. In the framework of the semiclassical theory, using the dipole approximation and rotating-wave approximation, the Hamiltonian H_I of the atomic system in the interaction picture is

$$H_I = \hbar[\delta|2\rangle\langle 2| + \Delta_p|3\rangle\langle 3| + (\delta + \Delta_s)|4\rangle\langle 4| - (g|3\rangle\langle 2| + \Omega_p|3\rangle\langle 1| + \Omega_s|4\rangle\langle 2| + \text{H.c.})]. \quad (1)$$

Including the relaxation terms for the system, the equations of motion for the density matrix of the system are

$$\begin{aligned}
\dot{\rho}_{11} &= i\Omega_p(\rho_{31} - \rho_{13}) + \Gamma_{31}\rho_{33} + \Gamma_{41}\rho_{44},\\
\dot{\rho}_{22} &= ig(\rho_{32} - \rho_{23}) + i\Omega_s(\rho_{42} - \rho_{24}) + \Gamma_{32}\rho_{33} + \Gamma_{42}\rho_{44},\\
\dot{\rho}_{33} &= i\Omega_p(\rho_{13} - \rho_{31}) + ig(\rho_{23} - \rho_{32}) - \Gamma_{31}\rho_{33} - \Gamma_{32}\rho_{33},\\
\dot{\rho}_{31} &= -(i\Delta_p + \gamma_{31})\rho_{31} + i\Omega_p(\rho_{11} - \rho_{33}) + ig\rho_{21},\\
\dot{\rho}_{32} &= -(i\Delta + \gamma_{32})\rho_{32} - i\Omega_s\rho_{34} + i\Omega_p\rho_{12} + ig(\rho_{22} - \rho_{33}),\\
\dot{\rho}_{42} &= -(i\Delta_s + \gamma_{42})\rho_{42} - ig\rho_{43} + i\Omega_s(\rho_{22} - \rho_{44}),\\
\dot{\rho}_{41} &= -[i(\Delta_s + \delta) + \gamma_{41}]\rho_{41} + i\Omega_s\rho_{21} - i\Omega_p\rho_{43},\\
\dot{\rho}_{43} &= [i(\Delta - \Delta_s) - \gamma_{43}]\rho_{43} + i\Omega_s\rho_{23} - i\Omega_p\rho_{41} - ig\rho_{42},\\
\dot{\rho}_{21} &= -(i\delta + \gamma_{21})\rho_{21} + ig\rho_{31} + i\Omega_s\rho_{41} - i\Omega_p\rho_{23},\\
1 &= \rho_{11} + \rho_{22} + \rho_{33} + \rho_{44}, \quad (2)
\end{aligned}$$

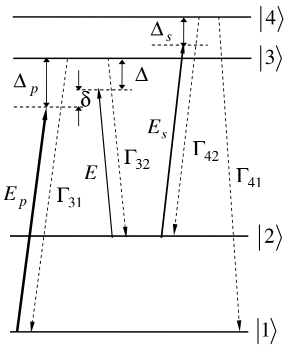

Fig. 1. Schematic diagram of the four-level atomic system in ARG configuration. The pumping field E_p, probe field E, and signal field E_s interact with the atomic transitions $|3\rangle$–$|1\rangle$, $|3\rangle$–$|2\rangle$, and $|4\rangle$–$|2\rangle$, respectively. Δ_p, Δ and Δ_s are detunings of the pumping, probe, and signal fields, respectively. Here, two-photon detuning of Raman resonance is $\delta = \Delta_p - \Delta$.

where $\Omega_p = \mu_{31}E_p/2\hbar$, $\Omega_s = \mu_{42}E_s/2\hbar$, and $g = \mu_{32}E/2\hbar$ are the real Rabi frequencies of the corresponding fields. Here γ_{ij} $(i, j = 1, 2, 3, 4)$ is the atomic coherence decay rate between the levels i and j.

For the Raman gain process, we consider that the atoms are initially populated in the ground state $|1\rangle$, and because the probe field is very weak, the density matrix above can be derived to the linear order of the probe field, and all orders of other fields. It is worthwhile to point out that the energy-level diagram in Fig. 1 is similar to the one used by Agarwal and Dasgupta for the superluminal pulse propagation [16]; thus the steady-state solution of Eq. (2) can be obtained numerically by using the complete set of density matrix equations. It is assumed that all atoms initially populate in level $|1\rangle$, and then there could be some populations in level $|2\rangle$ as two-photon detuning is small. However, the atoms in level $|2\rangle$ could be driven to level $|4\rangle$ by the pump effect of the signal field, and finally the atoms could return to level $|1\rangle$ by the spontaneous emission. As a result, the majority of atoms should stay in level $|1\rangle$ in the steady state. The induced atomic susceptibility experienced by the probe field is $\chi = 3\pi\mathcal{N}\Gamma_{32}\rho_{32}/g$, where $\mathcal{N} = N_0(\lambda/2\pi)^3$ is the scaled average atomic density, and N_0 and λ present the atomic density and wavelength of the probe field, respectively.

In order to create a grating, an intensity mask is added in the signal field, as shown in Fig. 2, and the Rabi frequency of signal field in cold atoms is chosen as

$$\Omega_s^2 = \frac{\gamma^2}{\sqrt{a\{x/D\} + b}}, \tag{3}$$

where $\{\ldots\}$ presents the fractional part of the function inside, γ is a scale to evaluate the signal Rabi frequency, and D is the grating period. We assume the parameters of a and b are x-independent constants. Therefore, it is found that $\chi = \chi(x)$ when Eq. (3) is substituted into Eq. (2). In the ARG system, we use Maxwell's equation to describe the propagation of the weak probe field with a small amplification. In the slowly varying envelope approximation, the equation in the steady state can be written as

$$\frac{-i}{2k}\frac{\partial^2 E}{\partial^2 x} + \frac{\partial E}{\partial z} = ik\chi E, \tag{4}$$

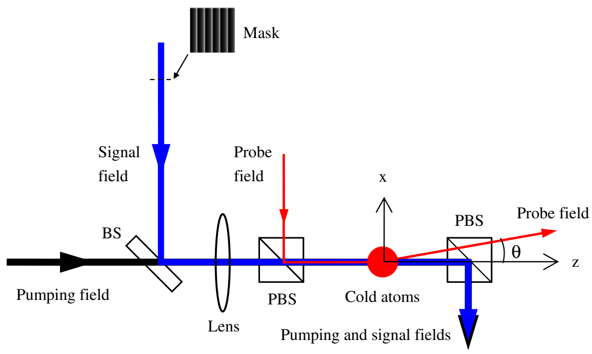

Fig. 2. (Color online) Schematic diagram of the beam setup for creating a blazed gain grating in an ultracold atomic medium. An intensity mask at the object plane of the lens creates an intensity image of the signal field in cold atoms at the image plane. The probe beam is diffracted at an angle θ by this grating. BS and PBS are the beam splitter and polarizing beam splitter, respectively.

where $k = 2\pi/\lambda$ is the wave vector of probe field. We use the one-photon absorption length of the probe field $\zeta = \lambda/6\pi^2\mathcal{N}$ as the unit of the length L of cold atoms, and use D as the unit for x. As a result, the wave equation becomes

$$\frac{-i}{\mathcal{N}_F}\frac{\partial^2 E}{\partial^2 x} + \frac{\partial E}{\partial z} = (-\alpha + i\beta)E, \tag{5}$$

where $\alpha = k\,\mathrm{Im}[\chi]$ and $\beta = k\,\mathrm{Re}[\chi]$ are the absorption and dispersion coefficients of the probe field. Here, $\mathcal{N}_F = 2kD^2/\zeta$ is the Fresnel number of a slit of width $2\sqrt{\pi}D$ at a distance ζ. In the case that $\mathcal{N}_F \gg 1$, the transverse term in Eq. (5) can be eliminated. Here, we use the typical parameters of ^{87}Rb D_1 line: Γ_{ij} $(i = 3, 4; j = 1, 2) = 2\gamma = 2\pi \cdot 5.75$ MHz and $\lambda = 795$ nm. For the atomic density $N_0 = 10^{13}$ cm^{-3} and grating period $D = 200\lambda$, it is found $\mathcal{N}_F \approx 6 \times 10^5$. Therefore, we can solve Eq. (5) analytically, and obtain the transmission function of probe field at $z = L$ as follows:

$$T(x) = e^{-\alpha(x)L}e^{i\beta(x)L}. \tag{6}$$

We assume that the input probe beam is a plane wave, and normalize its intensity to be equal to 1; thus the diffraction intensity distribution can be written as

$$I(\theta) = |E(\theta)|^2\frac{\sin^2(N\pi D\sin\theta/\lambda)}{N^2\sin^2(\pi D\sin\theta/\lambda)}, \tag{7}$$

where N is the number of spatial periods of the grating illuminated by the probe field, and θ is the angle between the direction of the diffracted beam and the z direction. In this theoretical model, the approximation of plane-wave beams is used to describe the grating, although an actual experiment should use Gaussian-like beams; this approximation has already been demonstrated to agree with the experimental results in the four-level atomic system [17]. In Eq. (7), the Fraunhofer diffraction of a single space period is

$$E(\theta) = \int_0^1 T(x)\exp(-ikDx\sin\theta)\mathrm{d}x. \tag{8}$$

3. RESULTS AND DISCUSSION

For the parameters $a = -1/5950$ and $b = 1/5920$ in Eq. (3), the periodic intensity image in the signal field and the Rabi frequency distribution of the signal field are depicted in Figs. 3(a) and 3(b), respectively. Here, we use γ_{ij} $(i = 3, 4; j = 1, 2) = 2.01\gamma$, $\gamma_{43} = 4.01\gamma$, $\gamma_{21} = 0.01\gamma$, $\Delta_p = 200\gamma$, $\Delta_s = 100\gamma$, $\delta = 0.1\gamma$, and $\Omega_p = 10\gamma$ in Eq. (2), and demonstrate the induced x-dependent transmission function in Fig. 3(c). We assume the interaction length of cold atoms is $L = 330$ μm, and these parameters are fixed in the rest of this paper. An investigation of Fig. 3(c) shows that the amplitude of probe filed is amplified periodically in space, and the corresponding phase modulation within a period can be 2π. It can be understood that the pumping field induces a Raman gain of probe field, and the signal field modulates the probe gain by changing two-photon detuning of Raman resonance. Therefore, the periodic intensity image in signal field makes the probe gain change periodically. Due to the Kramer–Kronig relations [18], the intensity mask in the signal field leads to a phase retardation, which has an approximate 2π periodic structure with an abrupt transition between the periods as shown in Fig. 3(c). The far-field diffraction pattern corresponding to the diffraction grating of Fig. 3(c) is depicted in Fig. 3(d). In Fig. 3(d), it is seen that the grating can deflect the probe beam through an angle of 5 mrad with the efficiency more than 100% into the first-order direction. For comparison, the diffraction pattern of the gain grating without the phase modulation is also demonstrated in Fig. 3(d). It is found that the gain grating plays no role in diffracting the probe beam, and the diffraction grating of Fig. 3(c) deflects the amplified probe beam into the first-order direction. Because Eq. (2) is derived to all orders of the signal field, the phase modulation induced by the intensity mask in the signal field is quasi-linear, as shown in Fig. 3(c); thus a small amount of probe energy is diffracted into an angle of 10 mrad. It is difficult to demonstrate a mask that can induce a linear phase modulation; however, it is clear that the majority of energy in the amplified probe beam has been deflected into the first-order direction, and the diffraction efficiency can approach 200%. Therefore, this kind of atomic grating is a blazed gain grating, which is a mixture of a gain grating and a phase grating. Since our scheme is based on the process of Raman gain, the probe beam at low light levels can also be manipulated, which may have great potential to be used as an all-optical switching and routing in the optical networking [14,15].

Based on the structure of blazed gain grating, a beam splitting with high efficiency can be obtained if we use a more sophisticated image in the signal field. The designed intensity image of signal field has a symmetric intensity distribution as shown in Fig. 4(a), and the corresponding signal Rabi frequency can be written as

$$\Omega_s^2 = \frac{\gamma^2}{\sqrt{a\{|x|/D\} + b}}. \tag{9}$$

Here, two symmetric domains have opposite blazed directions, and the corresponding signal Rabi frequency and induced x-dependent transmission function are shown in Figs. 4(b) and 4(c), respectively. We assume the input probe field has an amplitude uniform in the beam width of $12D$, and normalize its intensity to 1. Under these assumptions, the far-field angular intensity distribution of the diffracted probe beam can be given by

$$I(\theta) = \frac{1}{N^2}\left|\int_{-6}^{+6} T(x)\exp(-ikDx\sin\theta)\mathrm{d}x\right|^2. \tag{10}$$

We depict the Fraunhofer diffraction pattern induced by the intensity mask having two symmetric domains in Fig. 4(d),

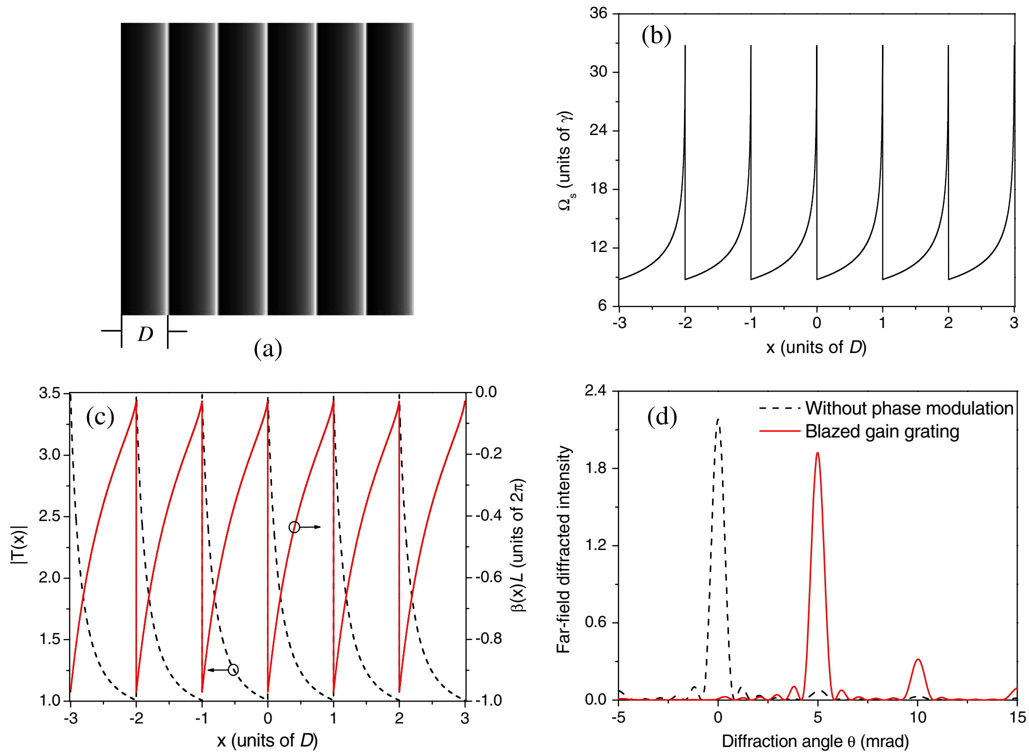

Fig. 3. (Color online) (a) Periodic intensity image in the signal field, and D is the spatial spacing. This image has finite width $6D$. (b) Numerical amplitude distribution of signal field according to the intensity image of Fig. 3(a). (c) Induced x-dependent amplitude (black dashed curve) and phase (red solid curve) of the transmission function $T(x)$. (d) Fraunhofer diffraction patterns for blazed gain grating of Fig. 3(c) (red solid curve), and the grating without phase modulation (black dashed curve).

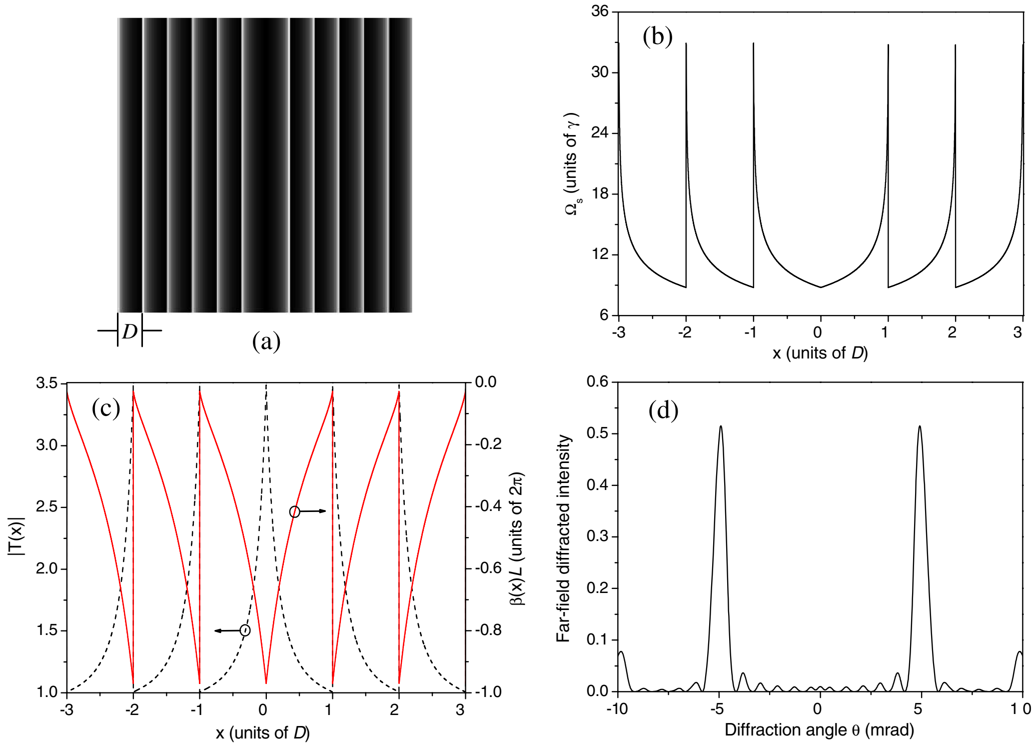

Fig. 4. (Color online) (a) Periodic intensity image that has two domains in the signal field to split the probe beam. The number of spatial periods in each domain is six. (b) Numerical amplitude distribution of signal field according to the intensity image of Fig. 4(a). For simplicity, only three periods in each domain are presented. (c) Amplitude (black dashed curve) and phase (red solid curve) of the transmission function $T(x)$ as a function of x, which is induced by the signal field in Fig. 4(b). (d) Fraunhofer diffraction pattern of the diffraction grating of Fig. 4(c).

and it is found that the incident probe beam is split into two beams of equal intensity, and the separated angle can nearly be 10 mrad. It is worthwhile to point out that the diffraction efficiency of each beam can be higher than 50%, which is higher than the efficiency of general beam splitting [12].

4. CONCLUSIONS

In conclusion, we theoretically demonstrated a blazed gain grating based on ARG in cold atoms. By using an intensity mask in the signal field, the induced atomic grating amplifies the probe beam, and deflects it with the efficiency higher than 100% through an angle of 5 mrad. This high diffraction efficiency indicates that a probe beam at low light levels can also be manipulated in our scheme, which may have some applications in the all-optical networks. When a more sophisticated intensity mask is used, our proposal can supply a further possibility of all-optical beam splitting.

REFERENCES

1. M. Fleischhauer, A. Imamoglu, and J. P. Marangos, “Electromagnetically induced transparency: optics in coherent media,” Rev. Mod. Phys. **77**, 633–673 (2005).
2. H. Y. Ling, Y. Q. Li, and M. Xiao, “Electromagnetically induced grating: homogeneously broadened medium,” Phys. Rev. A **57**, 1338–1344 (1998).
3. M. Mitsunaga and N. Imoto, “Observation of an electromagnetically induced grating in cold sodium atoms,” Phys. Rev. A **59**, 4773–4776 (1999).
4. L. E. E. de Araujo, “Electromagnetically induced phase grating,” Opt. Lett. **35**, 977–979 (2010).
5. Z. H. Xiao, S. G. Shin, and K. Kim, “An electromagnetically induced grating by microwave modulation,” J. Phys. B **43**, 161004 (2010).
6. R. G. Wan, J. Kou, L. Jiang, Y. Jiang, and J. Y. Gao, “Electromagnetically induced grating via enhanced nonlinear modulation by spontaneously generated coherence,” Phys. Rev. A **83**, 033824 (2011).
7. S. Q. Kuang, C. S. Jin, and C. Li, “Gain-phase grating based on spatial modulation of active Raman gain in cold atoms,” Phys. Rev. A **84**, 033831 (2011).
8. S. Q. Kuang, “Raman gain grating in an ultracold atomic medium,” Chin. Opt. **5**, 464–469 (2012).
9. L. Deng and M. G. Payne, “Gain-assisted large and rapidly responding Kerr effect using a room-temperature active Raman gain medium,” Phys. Rev. Lett. **98**, 253902 (2007).
10. K. J. Jiang, L. Deng, E. W. Hagley, and M. G. Payne, “Fast-responding nonlinear phase shifter using a signal-wave gain medium,” Phys. Rev. A **77**, 045804 (2008).
11. C. J. Zhu, C. Hang, and G. X. Huang, “Gain-assisted giant Kerr nonlinearity in a Λ-type system with two-folded lower levels,” Eur. Phys. J. D **56**, 231–237 (2010).
12. L. Zhao, W. H. Duan, and S. F. Yelin, “All-optical beam control with high speed using image-induced blazed gratings in coherent medium,” Phys. Rev. A **82**, 013809 (2010).
13. S. A. Carvalho and L. E. E. de Araujo, “Electromagnetically induced blazed grating at low light levels,” Phys. Rev. A **83**, 053825 (2011).
14. A. W. Brown and M. Xiao, “All-optical switching and routing based on an electromagnetically induced absorption grating,” Opt. Lett. **30**, 699–701 (2005).
15. A. Schilke, C. Zimmermann, and W. Guerin, “Photonic properties of one-dimensionally-ordered cold atomic vapors under conditions of electromagnetically induced transparency,” Phys. Rev. A **86**, 023809 (2012).
16. G. S. Agarwal and S. Dasgupta, “Superluminal propagation via coherent manipulation of Raman gain process,” Phys. Rev. A **70**, 023802 (2004).
17. M. V. Pack, R. M. Camacho, and J. C. Howell, “Transient of the electromagnetically-induced-transparency-enhanced refractive Kerr nonlinearity,” Phys. Rev. A **76**, 033835 (2007).
18. J. D. Jackson, *Classical Electrodynamics*, 2nd ed. (Wiley, 1975).